High Electron Transfer Efficiency of Titania Dioxide Nanotube for Low Potential Electrochemiluminescent Biosensing

Xuan Liu,[a] *Zhentao Hou*,[a] *Jianping Lei*,[a] *Huangxian Ju*,*[a] *Jingxuan Cai*,[b] *Jianyi Shen*[b]

[a] State Key Laboratory of Analytical Chemistry for Life Science, Department of Chemistry, Nanjing University, Nanjing 210093, P. R. China
[b] MOE Key Laboratory of Mesoscopic Chemistry, Department of Chemistry, Nanjing University, Nanjing 210093, P. R. China
*e-mail: hxju@nju.edu.cn

Received: July 18, 2011
Accepted: August 9, 2011

Abstract

Strong electrochemiluminescence (ECL) of titania dioxide nanotubes at physiological condition was observed, with relatively low cathodic potential due to its large surface area and high electron transfer efficiency. The coreactant of the ECL emission was proved to be H_2O_2, produced from the reduction of dissolved oxygen, leading to a mild ECL system for biosensing. Based on "coreactant inhibition" mechanism, the ECL quenchers could be measured by inhibiting the transformation of O_2 to H_2O_2. Using hemoglobin as a model, the quenched ECL emission followed Stern–Volmer equation in a wide linear range. Thus a novel methodology for detection of "coreactant inhibition"-related quencher could be developed with acceptable sensitivity.

Keywords: Titania dioxide nanotube, Electrochemiluminescence, Coreactant inhibition, Bioanalysis, Hemoglobin

DOI: 10.1002/elan.201100379

Electrogenerated chemiluminescence (ECL) behaviors of semiconductor nanoparticles have attracted considerable interest due to their potential applications in bioanalysis and energy fields [1]. Upon the understanding of ECL mechanisms and the development of multitudinous coreactants, many new ECL systems of quantum dots (QDs) have been proposed by coreactant enhancing [2,3] or signal quenching [4]. However, the overwhelming used QDs ECL emitters were focused on II-VI QDs, which were of great biotoxicity and suffered instability during storage even at 4 °C. Recently, many nanostructures with low biotoxicity such as Au_{25} [5] and Ag [6] nanoclusters, C-dots [7], and ZnO [8] and TiO_2 nanoparticles (NPs) [9] have shown excellent ECL emission and been used as ECL emitters. However, most of these nano-ECL emitters show relatively high emission potential and need strong oxidant $S_2O_8^{2-}$ as coreactant to produce ECL signal, which greatly increase the occurrence of undesired reaction and are adverse for both bioanalysis and fabrication of energy devices. Here, a novel nano-ECL emitter, TiO_2 nanotube (TNT) with lower biotoxicity, was suggested to overcome these limits.

TiO_2 nanoparticles have been extensively used as advanced photocatalytic materials. The photoluminescent behaviors of TiO_2 nanostructures have been widely reported [10]. Compared with general QDs, TNT possesses large surface areas and narrower surface band gap, which will produces high quantum transfer efficiency, higher ECL efficiency and lower emission potential [11,12]. However, its ECL characteristics and applications have rarely been investigated. This work observed a strong ECL emission from TNT in air-saturated neutral buffer with a relatively low potential, approximately 500 mV more positive than those reported cathodic ECL systems using TiO_2 NPs [9] or TNT [13,14] as ECL emitters. The ECL mechanism was proved to be a coreactant-induced process. The coreactant H_2O_2 was produced from the reduction of dissolved oxygen, leading to a mild ECL system without assistance of any other strong oxidant. A "coreactant inhibition" mechanism was further proposed to develop a novel methodology for ECL detection of quenchers using hemoglobin (HB) as a model.

The powder X-ray diffraction (XRD) spectrum showed an anatase crystal form of the as-prepared TNT (Figure 1A). Its high-resolution transmission electron microscope (HRTEM, JEM-2100, JEOL) showed a nanotube structure with a length of ~90 nm and a diameter of 12 nm (Inset, Figure 1B). The formed TNT film exhibited a uniform morphology with the homogeneous aggregation size maintaining the original shape of the TNT (Figure 1B).

Compared with the bare electrode, the TNT, P25 and anatase TiO_2 NPs modified electrodes showed lower electron transfer impedance, while rutile TiO_2 NPs modified electrode showed higher value (Figure 2A). The TNT modified electrode possessed the highest electron transfer efficiency among the four nanostructures of TiO_2. It could be attributed to the large surface/volume ratio of TNT and the high quantum efficiency of TNT due to the unpassivated surface and narrow band gap, which was

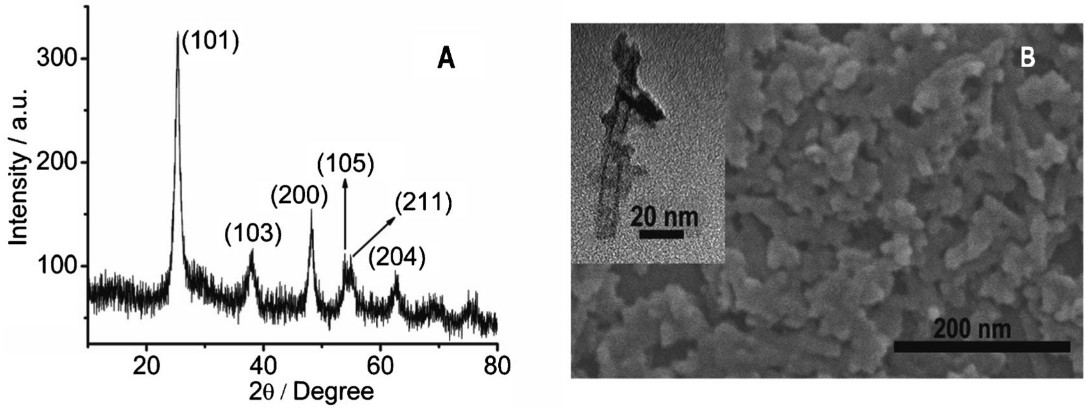

Fig. 1. (A) XRD pattern of TNT and (B) scanning electron microscopic (SEM) image of TNT/ITO. Inset: HRTEM of TNT.

beneficial to the ECL emission at relatively lower peak potential.

As expected, the ECL intensities of the four TiO_2 nanostructures showed a consistent pattern with the EIS (Figure 2B). During the cathodic scan, the TNT modified indium tin oxide (ITO) electrode (TNT/ITO) showed a strong ECL emission at ~0.90 V (vs. Ag/AgCl) in air-saturated pH 7.5 Tris-HCl buffer (curve a). Compared to the P25, anatase and rutile TiO_2 NPs, the TNT/ITO showed the maximum ECL intensity and the lowest emission peak potential. Furthermore, different from the traditional II-VI QDs, the pH of detection solution did not obviously affect the ECL intensity of TNT/ITO, while the emission peak negatively shifted with the increasing solution pH (Figure 2C), which was similar with the electrochemical behavior of TiO_2 nanostructure [15]. The rela-

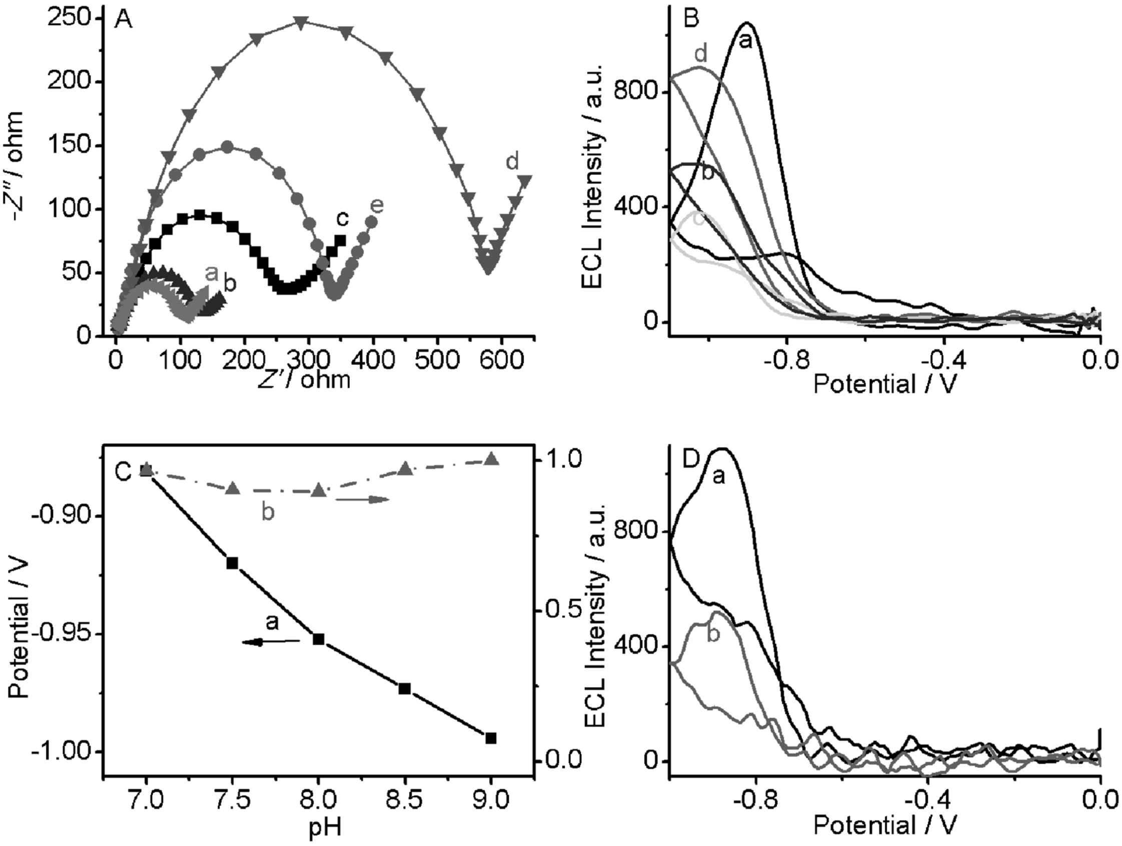

Fig. 2. (A) Electrochemical impedance spectra (EIS) of TNT (a), P25 (b), anatase (c) and rutile (d) TiO_2 NPs modified and bare (e) ITO electrodes in 0.1 M KCl containing 5 mM $[Fe(CN)_6]^{3-/4-}$. (B) Cyclic ECL curves of TNT (a), TiO_2 NPs (b), anatase (c) and rutile (d) modified ITO, and (C) plots of ECL peak potential (a) and intensity (b) of TNT/ITO vs. pH of air-saturated buffer. (D) Cyclic ECL curves of TNT/ITO in air-saturated (a) and degassed (b) detection solution.

tive standard deviation (*RSD*) for five parallel measurements (intraassay) of ECL emission with one TNT/ITO was 2.6%, indicating a good stability. The ECL detection of five TNT/ITOs fabricated independently (interassay) showed the RSD of 2.7%, giving an acceptable fabricated reproducibility of the TNT/ITO.

Although lower emission peak potential could be obtained at lower pH, pH 7.5 was finally selected for the following application considering the acceptable potential and bioanalytical requirement.

To further applying the ECL signal of TNT/ITO, the emitting mechanism was firstly discussed. In the detection solution, dissolved oxygen was the only assistant to produce the strong ECL emission. During the cathodic scan, the self-produced H_2O_2 from reduction of dissolved O_2 acted as the coreactant to form the hole injected TiO_2 ($TiO_2(h^+)$), which could then collide with electron injected TiO_2 ($TiO_2(e^-)$), the electro-reduction product of TiO_2, to produce the excited TiO_2* and ECL emission. This mechanism could be verified by adding H_2O_2 in air-free pH 7.5 Tris-HCl buffer, in which the TNT/ITO showed the same ECL emission. In addition, the ECL intensity of TNT/ITO was sharply decreased after the dissolved O_2 was removed from the detection solution by bubbled with N_2 for 20 min (Figure 2D).

Ferriporphyrin (FePP) could quench the ECL emission of TNT/ITO by catalyzing the reduction of dissolved O_2 to H_2O at -0.455 V (vs. Ag/AgCl, Figure 3A), during which H_2O_2 could not be produced [16], leading to dramatically decreased ECL intensity (Figure 3B). Furthermore, the transition metal ions, such as Ni^{2+}, Cu^{2+}, Co^{2+}, Fe^{2+}, which could catalyze the decomposing of H_2O_2 to O_2 [17], also quenched the ECL emission of TNT/ITO with high efficiency (Figure 3B). Common proteins, such as bovine serum albumin (BSA) and horseradish peroxidase (HRP, 250 U/mg solid, Sigma) did not obviously affect the ECL emission of TNT/ITO. These phenomena indicated that the dissolved O_2 participated the ECL emission as a precursor of the self-produced coreactant H_2O_2. Thus a novel analytical methodology for quencher-related detection could be constructed by inhibiting the transformation of O_2 to H_2O_2, defined as a "coreactant inhibition" mechanism.

Considering the importance of HB detection in health care, it was selected as a model. When HB was added into the detection solution, O_2 was absorbed by its subunits, thus could not be reduced on the electrode surface to produce the coreactant of H_2O_2. As a result the ECL of TNT/ITO was quenched effectively (Figure 4A). Based on the quenching effect, a rapid analytical method for HB detection could be developed. The plot of the ratio of initial ECL intensity I_0 to the intensity I at a given HB concentration vs. HB concentration ranging from 0 to 2 mg mL^{-1} showed a linear relation ($R=0.995$, Figure 4B). The limit of detection was 4 μg mL^{-1} at an ECL quenching degree of 10%.

The cathodic ECL of TNT, a novel nano-ECL emitter with low biotoxicity and large surface areas, is observed at a relatively low emission potential in neutral system. The coreactant has proved to be H_2O_2, which is produced from the reduction of dissolved O_2. The efficient ECL emission of the mild nano-ECL system can be quenched by compounds such as HB via a "coreactant inhibition" mechanism, producing new methodology for sensitive ECL detection of quencher-related analytes. More bioanalytical strategies could be expected to be designed using this novel nano-ECL system, such as enzymic biosensing [12], small molecule detection [13], immunoassay [19] or cell detection [20]. Furthermore, by combining TiO_2 NPs with different ECL emission potentials, simultaneous ECL analysis for multi-targets by potential resolution could be carried out. These results provide a potential alternative for developing novel nano-ECL emitters and significantly extend the application of ECL technique in bioanalysis.

Experimental

The commercial P25 TiO_2 NPs (30 nm, S_{BET} 52 m^2 g^{-1}) were purchased from Degussa. Deionized water and 0.1 M Tris-HCl buffer containing 0.1 M KNO_3 were used

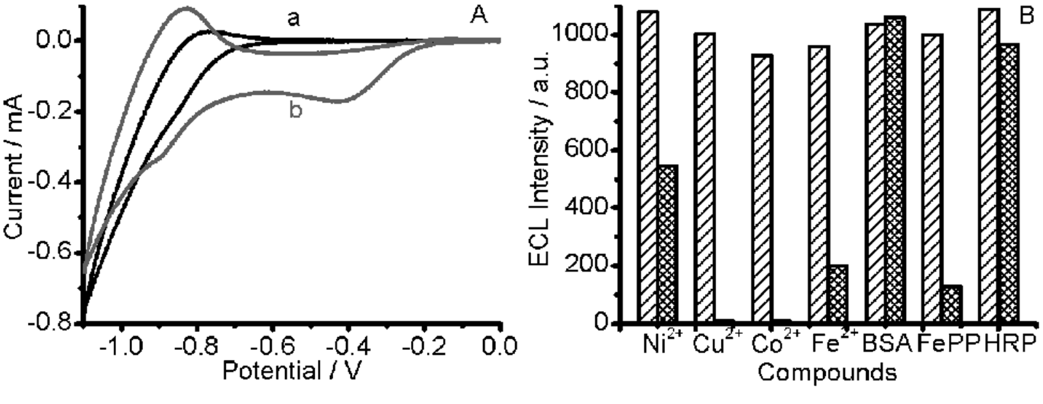

Fig. 3. (A) CV curves of TNT/ITO in absence (a) and presence (b) of 10 μM FePP, and (B) ECL intensities of TNT/ITO in absence (diagonal) and presence (cross) of 0.1 mM Ni^{2+}, Cu^{2+}, Co^{2+}, Fe^{2+}, 1 mg mL^{-1} BSA, 10 μM FePP and 100 μg mL^{-1} HRP.

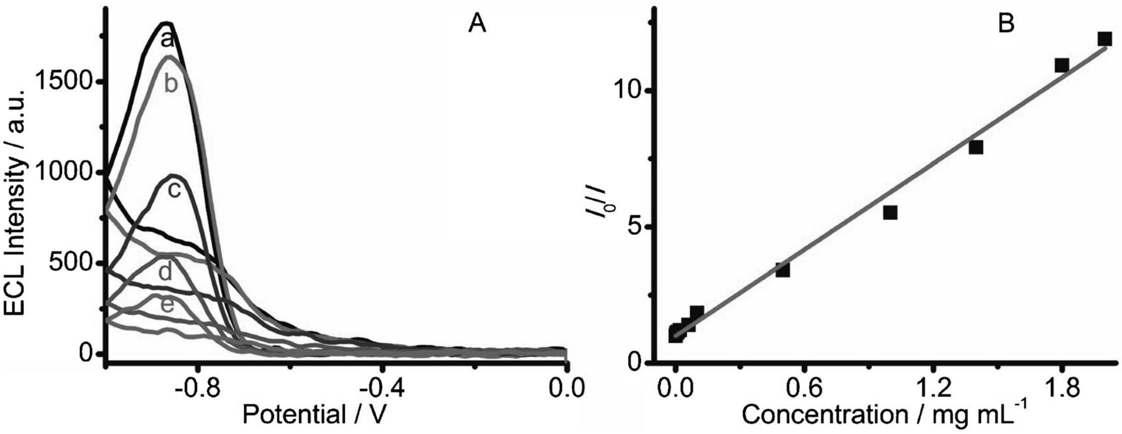

Fig. 4. (A) Cyclic ECL curves of TNT/ITO in air-saturated buffer containing (a) 0 and (b) 4 µg mL^{-1}, (c) 0.1, (d) 0.5 and (e) 1.0 mg mL^{-1} HB, and (B) plot of ECL intensity vs. HB concentration.

throughout the work. All reagents were of analytical grade. The electrochemical and ECL measurements were performed on an MPI-E analytical system (Xi'an Remex Analytical Instrument Ltd. Co.) at room temperature with an ITO working electrode (1 cm × 3 cm with 1 cm × 0.5 cm for TNT modification), a platinum counter electrode and a Ag/AgCl (saturated KCl solution) reference electrode. The observation window for ECL was placed in front of the photomultiplier tube biased at 1000 V. XRD pattern was collected on Philips X' Pert Pro diffractometer (Netherlands). SEM image of the TNT film (TNT/ITO) was obtained using a Hitachi S-4800 scanning electron microscope (Japan). The EIS were recorded on a PGSTAT30/FRA2 system (Autolab, Netherlands).

TNT was prepared via hydrothermal synthesis according to [18]. Briefly, 0.9 g commercial TiO_2 nanoparticles were dispersed in 30 mL of 10 M NaOH and stirred for 30 min. The mixture was heated at 403 K for 24 h. The obtained paste was washed with 0.1 M and 0.05 M HNO_3, sequentially, and then distilled water at 318 K to neutral. The obtained white paste was finally dried at 313 K overnight and then calcined at 673 K for 1 h. The as-prepared TNT was stored in dark at room temperature. The TNT film was prepared by dropping 20 µL of 2 mg mL^{-1} TNT suspension on ITO electrode and dried in air in the dark.

Acknowledgements

This work was financially supported by the *National Natural Science Foundation of China* (920875044, 20821063) and the *Natural Science Foundation of Jiangsu* (BK2008014).

References

[1] W. J. Miao, *Chem. Rev.* **2008**, *108*, 2506.
[2] G. Z. Zou, H. X. Ju, *Anal. Chem.* **2004**, *76*, 6871.
[3] X. F. Wang, Y. Zhou, J. J. Xu, H. Y. Chen, *Adv. Funct. Mater.* **2009**, *19*, 1444.
[4] X. Liu, H. X. Ju, *Anal. Chem.* **2008**, *80*, 5377.
[5] L. L. Li, H. Y. Liu, Y. Y. Shen, J. R. Zhang, J. J. Zhu, *Anal. Chem.* **2011**, *83*, 661.
[6] I. Díez, M. Pusa, S. Kulmala, H. Jiang, A. Walther, A. S. Goldmann, A. H. E. Müller, O. Ikkala, R. H. A. Ras, *Angew. Chem. Int. Ed.* **2009**, *48*, 2122.
[7] L. Y. Zheng, Y. W. Chi, Y. Q. Dong, J. P. Lin, B. B. Wang, *J. Am. Chem. Soc.* **2009**, *131*, 4564.
[8] R. X. Zhang, L. Z. Fan, Y. P. Fang, S. H. Yang, *J. Mater. Chem.* **2008**, *18*, 4964.
[9] Z. Y. Lin, Y. Liu, G. N. Chen, *Electrochem. Commun.* **2008**, *10*, 1629.
[10] J. M. Notestein, E. Iglesia, A. Katz, *Chem. Mater.* **2007**, *19*, 4998.
[11] N. Myung, Y. Bae, A. J. Bard, *Nano Lett.* **2003**, *3*, 1053.
[12] X. Liu, L. X. Cheng, J. P. Lei, H. Liu, H. X. Ju, *Chem. Eur. J.* **2010**, *16*, 10764.
[13] J. X. Li, L. X. Yang, S. L. Luo, B. B. Chen, J. Li, H. L. Lin, Q. Y. Cai, S. Z. Yao, *Anal. Chem.* **2010**, *82*, 7357.
[14] L. F. Chen, L. L. Lu, Y. Mo, Z. M. Xu, S. P. Xie, H. Y. Yuan, D. Xiao, M. M. F. Choi, *Talanta* **2011**, *85*, 56.
[15] B. P. Nelson, R. Candal, R. M. Corn, M. A. Anderson, *Langmuir* **2000**, *16*, 6094.
[16] H. Shin, D. H. Lee, C. Kang, K. D. Karlin, *Electrochim. Acta* **2003**, *48*, 4077.
[17] S. Rachmilovich-Calis, A. Masarwa, N. Meyerstein, D. Meyerstein, R. Eldik, *Chem. Eur. J.* **2009**, *15*, 8303.
[18] J. W. Liu, Y. C. Fu, Q. Sun, J. Y. Shen, *Microporous Mesoporous Mater.* **2008**, *116*, 614.
[19] J. Qian, C. Y. Zhang, X. D. Cao, S. Q. Liu, *Anal. Chem.* **2010**, *82*, 6422.
[20] E. Han, L. Ding, H. Z. Lian, H. X. Ju, *Chem. Commun.* **2010**, *46*, 5446.